

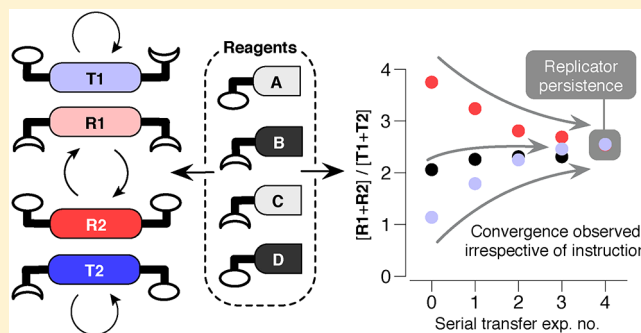
# Compositional Persistence in a Multicyclic Network of Synthetic Replicators

Jürgen Huck, Tamara Kosikova,<sup>†</sup> and Douglas Philp<sup>\*,†</sup>

School of Chemistry and EaStCHEM, University of St Andrews, North Haugh, St Andrews, Fife KY16 9ST, U.K.

## Supporting Information

**ABSTRACT:** The emergence of collections of simple chemical entities that create self-sustaining reaction networks, embedding replication and catalysis, is cited as a potential mechanism for the appearance on the early Earth of systems that satisfy minimal definitions of life. In this work, a functional reaction network that creates and maintains a set of privileged replicator structures through auto- and cross-catalyzed reaction cycles is created from the pairwise combinations of four reagents. We show that the addition of individual preformed templates to this network, representing instructions to synthesize a specific replicator, induces changes in the output composition of the system that represent a network-level response. Further, we establish through sets of serial transfer experiments that the catalytic connections that exist between the four replicators in this network and the system-level behavior thereby encoded impose limits on the compositional variability that can be induced by repeated exposure to instructional inputs, in the form of preformed templates, to the system. The origin of this persistence is traced through kinetic simulations to the properties and inter-relationships between the critical ternary complexes formed by the auto- and crosscatalytic templates. These results demonstrate that in an environment where there is no continuous selection pressure the network connectivity, described by the catalytic relationships and system-level interactions between the replicators, is persistent, thereby limiting the ability of this network to adapt and evolve.



## INTRODUCTION

The emergence of life on Earth signaled the appearance of self-sustaining systems that could harness nonlinear processes in the pursuit of complex functions, such as replication, self-sorting, ensemble-based control mechanisms, and, ultimately, chemical evolution. It has been suggested<sup>1</sup> that small organic molecules could create functional networks through sets of auto- and cross-catalyzed reaction cycles that, in turn, could select and amplify favored components. This process would lead to the appearance of sets of privileged molecular structures that are persistent within these networks. The mechanisms by which these networks could emerge are the subject of significant debate,<sup>2</sup> and developing an understanding of processes that can transition groups of simple chemical entities into more complex systems is a key target for the emerging field<sup>3</sup> of systems chemistry.

Minimal replication processes are often placed<sup>2d,e,3a,f</sup> at the center of these transitions and, consequently, may represent an important requirement for the appearance on Earth of systems that satisfy minimal definitions<sup>4</sup> of life. Therefore, the emergence of persistent sets of molecules that can establish and manage replication within small chemical networks is a critical prerequisite for the appearance of such systems. Experimental synthetic replicating systems,<sup>5</sup> developed by us<sup>6</sup> and others,<sup>7–9</sup> have demonstrated that template-driven replication is possible in synthetic systems using a variety of

chemistries: from oligonucleotides<sup>7</sup> and peptides<sup>8</sup> to small organic molecules.<sup>6,9</sup> In isolation, individual replicators behave in predictable ways and are capable of processing<sup>10</sup> pools of reagents to direct and amplify their own formation. However, the presence of several interconnected catalytic processes within the same reaction network can give rise to significantly more complex phenomena, such as programmed outputs,<sup>6b,8e,11</sup> feedback loops,<sup>12</sup> and oscillations.<sup>13</sup> In the context of “metabolism-first” scenarios<sup>1,2d</sup> for the emergence of life, network regulation in terms of composition is required to ensure the persistence of the key chemical constitutions that sustain the network. While taking inspiration from the complexity of natural systems, we wish to explore the persistence<sup>13a,14</sup> of replicators in networks through systems that possess both structural and interactional simplicity in terms of their chemical components. Such systems can be analyzed and characterized comprehensively, thereby providing a methodological grounding for the development and understanding, both experimental and theoretical of the processes relevant to the origin of life.

A prerequisite for examining replicator persistence is a network of interconnected and interdependent replication cycles in which the replicating templates compete with each

Received: June 24, 2019

Published: August 12, 2019

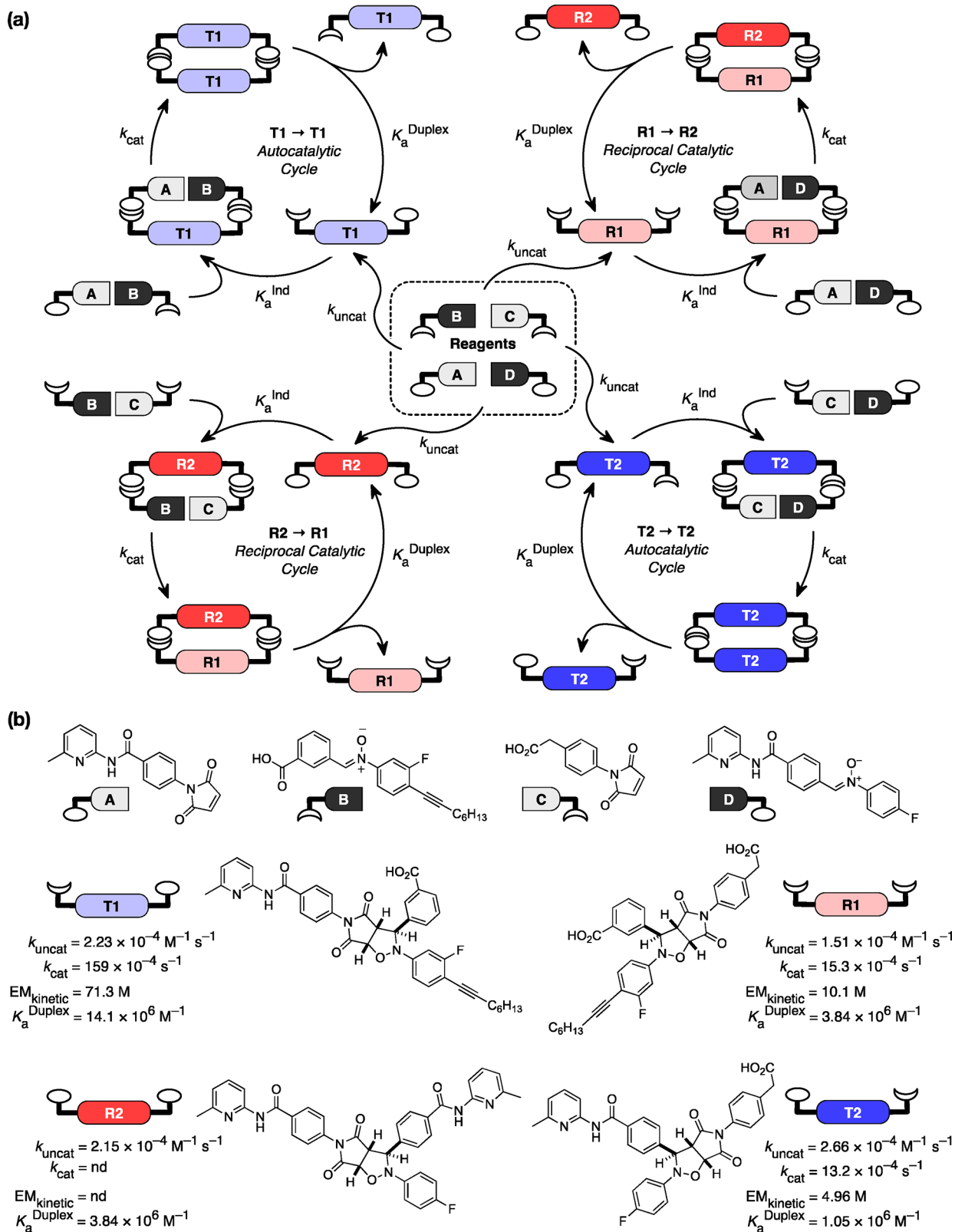


**Figure 1.** Reagents A to D react to create a multicyclic network of interdependent replicators. (a) Pairwise reactions of four reagents (A to D, center) form four replicators, T1, T2, R1, and R2 through bimolecular pathways ( $k_{\text{uncat}}$ ). Minimal replicators T1 and T2 are capable of assembling the reagents required to copy themselves and accelerating the reaction between them ( $k_{\text{cat}}$ ;  $\text{EM}_{\text{kinetic}} = k_{\text{cat}}/k_{\text{uncat}}$ ), completing autocatalytic cycles (top left and bottom right). Reciprocal replicators R1 and R2 are capable of assembling the reagents required to create their complementary partner and then accelerating the reaction between them ( $k_{\text{cat}}$ ), completing reciprocal catalytic cycles (top right and bottom left). (b) Chemical structures of reagents A to D and the replicators (T1, T2, R1, and R2) derived from these reagents. Key kinetic and thermodynamic parameters for each replicator are given next to the relevant structure. nd indicates parameters that could not be determined experimentally as a result of the limited solubility of R1 in  $\text{CDCl}_3$  following its purification.

other for the chemical building blocks necessary for their construction. The building blocks themselves must possess recognition sites that can be used to direct the requisite replication processes and reaction sites that can deliver a programmed pattern of reactivity. To this end, we identified a set of four reagents, shown at the center of Figure 1. These four reagents, A to D, are grouped such that each individual reagent possesses one of two possible recognition sites and one of two possible reactive elements. Thus, reagent A and reagent B possess recognition sites and reactive elements that are complementary to each other, and their combination gives rise to self-replicator T1, which is capable of directing its own formation through an autocatalytic cycle (Figure 1a, top left). Reagents C and D have a similar relationship and afford self-replicator T2, which is also capable of directing its own formation through an autocatalytic cycle (Figure 1a, bottom right). By contrast, reagents B and C possess complementary reactive elements, but identical recognition sites. The combination of these two reagents affords template R1 (Figure 1a, top right), which bears identical recognition sites and so cannot catalyze its own formation directly. Similarly, reagents A and D also possess complementary reactive elements, but identical recognition sites and their combination affords template R2 (Figure 1a, bottom left), which also cannot catalyze its own formation directly. However, taken together, R1 and R2 are mutually complementary in terms of recognition and can therefore participate (Figure 1a, top right and bottom left) in two cross-catalytic cycles whereby R1 catalyzes the formation of R2 and *vice versa*. These relationships represent a reciprocal replication cycle.

The network shown in Figure 1a possesses the minimal lexicon of intermolecular interactions and reactions required to create a tightly coupled reaction network that contains both self-replicators (autocatalytic, T1 and T2) and reciprocal replicators (cross-catalytic, R1 and R2). Since these replicators must construct themselves from a common reagent pool (A to D), we expect that the product distribution expressed by this network will be amenable to perturbation by the addition<sup>5,6</sup> of the instructional templates (T1, T2, R1, and R2).

In order to implement this network experimentally, it is necessary to design suitable building blocks to assume the roles of reagents A to D. To this end, we exploited our previous work in the design and construction of both self- and reciprocal replicators<sup>6,10,15</sup> to identify the four compounds shown in Figure 1b. This group of compounds contains two maleimides (A and C) and two nitrones (B and D). Pairwise 1,3-dipolar cycloaddition reactions afford two self-replicators, T1 and T2, and two reciprocal replicators, R1 and R2. A key consideration in the design of the network components is the ease with which the composition of the reaction mixture can be determined experimentally. To this end, a fluorine atom is present in both B and D and, thus, a fluorine atom is also present in each of the templates, allowing  $^{19}\text{F}\{^1\text{H}\}$  NMR spectroscopy to be used as the analytical tool for this network. The large dispersion in  $^{19}\text{F}$  chemical shifts ensures that all of the critical compounds present in the network can be identified and quantified unambiguously.

In this work, we describe the properties of the tightly coupled reaction network built from this set of simple synthetic replicators and demonstrate that the population distribution within this network can be influenced in predictable ways by the addition of preformed replicator templates as instructions. The system-level<sup>16</sup> properties expressed by this network are

such that the global population ratios of the replicators within the network are resistant to changes brought about by external pressure. This resistance is demonstrated to be a consequence of the catalytic relationships encoded by the network.

## RESULTS AND DISCUSSION

**Network Characterization.** Initially, we characterized the replicating behavior of each of the individual templates experimentally and used published protocols<sup>6,10,15</sup> for the analyses of experimental data from replicators to extract the key kinetic and thermodynamic parameters for each template (Figure 1b; for details, see the Supporting Information). Having characterized the replicators in isolation, we next assessed the performance of the complete network. A solution of reagents A to D in  $\text{CDCl}_3$  ( $[\text{A}] = [\text{B}] = [\text{C}] = [\text{D}] = 10 \text{ mM}$ ) was prepared, and the formation of the replicators, T1, T2, R1, and R2, was monitored by 470 MHz  $^{19}\text{F}\{^1\text{H}\}$  NMR spectroscopy (Figure 2a) over a period of 44 000 s. From the concentration–time profiles for the species present in the network (Figure 2a), it is clear that the rates of formation of the reciprocal replicators, R1 and R2, are higher than those for the self-replicators, T1 and T2, and that the rates of formation within each class of replicators are tightly coupled. These differential reaction rates for the two classes of replicators result in a 1.9:1 preference (Figure 2b, No T) for the formation of R1 and R2 over T1 and T2.

In general, the introduction of the other reciprocal replicator template (R2, Figure 4b) or a self-replicating template to a reaction mixture represents<sup>5,6</sup> an instruction to up-regulate the production of the added template. Similarly, the introduction of a reciprocal replicating template to a reaction mixture represents an instruction to up-regulate the production of the replicator that is complementary to the added template. In order to investigate the ability of a template-based instruction to alter the output of our replicator network, we performed a series of experiments in which a solution of the reagents A to D in  $\text{CDCl}_3$  ( $[\text{A}] = [\text{B}] = [\text{C}] = [\text{D}] = 10 \text{ mM}$ ) was instructed by the addition of 20 mol % of either R2, T1, or T2 at  $t = 0$ . The concentrations of the four replicators, T1, T2, R1, and R2, were then determined by 470 MHz  $^{19}\text{F}\{^1\text{H}\}$  NMR spectroscopy after a period of 44 000 s. These experiments (Figure 2b) reveal significant changes in the concentrations of all of the replicators in each experiment compared to that where no replicator instruction has been added.

When the network is instructed by the addition of R2, the preference for the formation of the reciprocal replicators overall is increased to 4.2:1. However, the replicator that is up-regulated most strongly is, in fact, R1, i.e., the complementary partner of the instructing template R2, reflecting the instruction given to the system: make R1. The reciprocal, cross-catalytic relationship between R1 and R2 ensures that the increase in production of R1 arising from the presence of the R2 instruction also results in an increase in the concentration of the instructing template itself. By contrast, when the network is instructed by the addition of self-replicator T1, the preference for the formation of the reciprocal replicators is erased almost entirely: the ratio of the reciprocal replicators (R1 and R2) to the self-replicators (T1 and T2) is now 1.1:1. In this case, however, the replicator that is up-regulated the most is the instructing template T1 itself, reflecting the fact that this template is capable of directing its own formation only. Similar results are obtained when the network is instructed with self-replicator T2: the

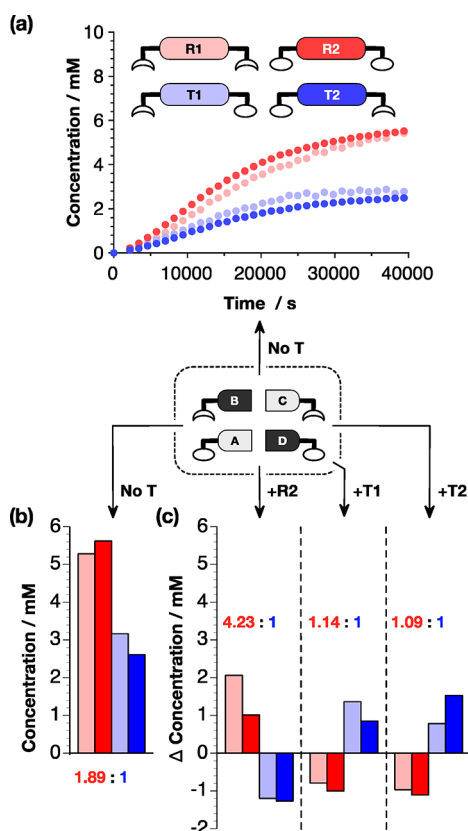


**Figure 2.** Individual replicators act as instructions to the multicyclic network. (a, b) In the absence of an instructional template, reactions of A to D within the network shown in Figure 1 ( $[A] = [B] = [C] = [D] = 10$  mM in  $CDCl_3$  at 283 K, monitored by 470 MHz  $^{19}F\{^1H\}$  NMR spectroscopy) result in the formation of a mixture of replicators. The combined concentrations of reciprocal replicators (R1 and R2, pink and red circles (a) and pink and red bars (b)) are approximately twice those of the autocatalytic replicators (T1 and T2, light and dark blue circles (a) and light and dark blue bars (b)). (c) The addition of 20 mol % of specific replicators, introduced as network instructions, at the start of the reaction between reagents A to D elicits both predictable and system-level changes in the composition of the reaction network after 44 000 s (12.2 h). The addition of a reciprocal replicator (+R2) increases the concentrations of both reciprocal replicators, and the addition of one autocatalytic replicator (either + T1 or + T2) increases the concentrations of both autocatalytic replicators. The poor solubility of R1 in  $CDCl_3$  following its purification precluded its use as instruction in template-directed experiments.

ratio of the reciprocal replicators (R1 and R2) to the self-replicators (T1 and T2) is also 1.1:1.

The effects of instruction are also reinforced by the connectivity of the reaction network created by the four replicators. For example, instructing the system with T1 up-regulates not only the production of this self-replicator within the network but also the other self-replicator T2. This observation is, at first sight, odd, since there is no explicit cross-catalytic relationship between T1 and T2. However, this system-level effect can be understood readily by considering the effect of the T1 added on the rates of the various reaction processes that form the replicators within the network. Self-replicator T1 is constructed from building blocks A and B, and the addition of T1 at the start of the experiment will increase the initial rate of their consumption. In the absence of appropriate added templates, the other replicators, T2, R1, and

R2, all rely on bimolecular reactions to form either themselves or their complementary partner before the respective catalytic cycles can become effective. In this context, the reciprocal replicators R1 and R2 also require building blocks A and B, respectively. Since these two building blocks are consumed at significantly increased initial rates in the presence of added T1 through the autocatalytic cycle that T1 exploits to form itself, the bimolecular rates for the formation of R1 and R2 are decreased significantly. By contrast, self-replicator T2 actually benefits from these changes in the rates of formation of R1 and R2, since T2 requires building blocks C and D only. Consequently, T2 will be formed at a comparatively higher initial rate than either R1, which requires B, or R2, which requires A. Therefore, the reagent flux through the autocatalytic cycle involving T2 becomes significant at an earlier time point than the cross-catalytic cycles involving the reciprocal replicators R1 and R2. Since R1 and R2 also require building blocks C and D for their formation, this small advantage afforded to T2 through the differences in the bimolecular rates is amplified by the autocatalytic formation of T2 and results in the observed up-regulation of T2 at the expense of R1 and R2.

**Replicator Persistence within the Network.** This replicator network shows predictable responses to direct template inputs and, additionally, exhibits system-level behavior that arises as a result of interconnections between the species within it. These features could lead to the appearance of sets of privileged molecular structures that are persistent within this network. The mechanisms by which such networks could emerge are the subject of significant debate,<sup>2</sup> and developing an understanding of processes that can transition groups of simple chemical entities into more complex systems is a key target for the emerging field<sup>3</sup> of systems chemistry. On the early Earth, such networks would have been subject<sup>17</sup> to pressures from compositional changes in the reagent feed and environmental changes. These pressures would have challenged the stability and persistence of potentially fragile replicator networks. In order to establish experimentally the effect of such events on the replicator composition within this network, we designed a set of serial transfer experiments<sup>18</sup> (Figure 3) that subjected the replicator network to simulated environmental changes.

First, we wished to explore how our network responded to environmental events in which a fresh input of the starting materials only was provided. The intrinsic kinetic properties of the network generate an approximately 2:1 preference for the reciprocal replicators R1 and R2, and we wished to explore whether this natural bias was stable under the environmental conditions described. Accordingly, we performed an initial experiment in which a solution of the reagents A to D in  $CDCl_3$  was prepared ( $[A] = [B] = [C] = [D] = 10$  mM, Figure 3a, box labeled F). No additional instructional template was added to this solution at the start of the reaction. The formation of the minimal replicators, T1 and T2, and the reciprocal replicators, R1 and R2, was assayed by 470 MHz  $^{19}F\{^1H\}$  NMR spectroscopy after complete consumption of starting materials. After this time, the ratio of reciprocal replicators to self-replicators ( $[RR]/[SR] = ([R1] + [R2])/([T1] + [T2])$ ) in this sample (Figure 3a, cycle 0) was 2.06:1. Next, the mixture of products obtained at the end of cycle 0 was used as an instructional input for cycle 1. This process simulates pressures on the network arising from compositional changes in the reagent feed and also environmental changes.



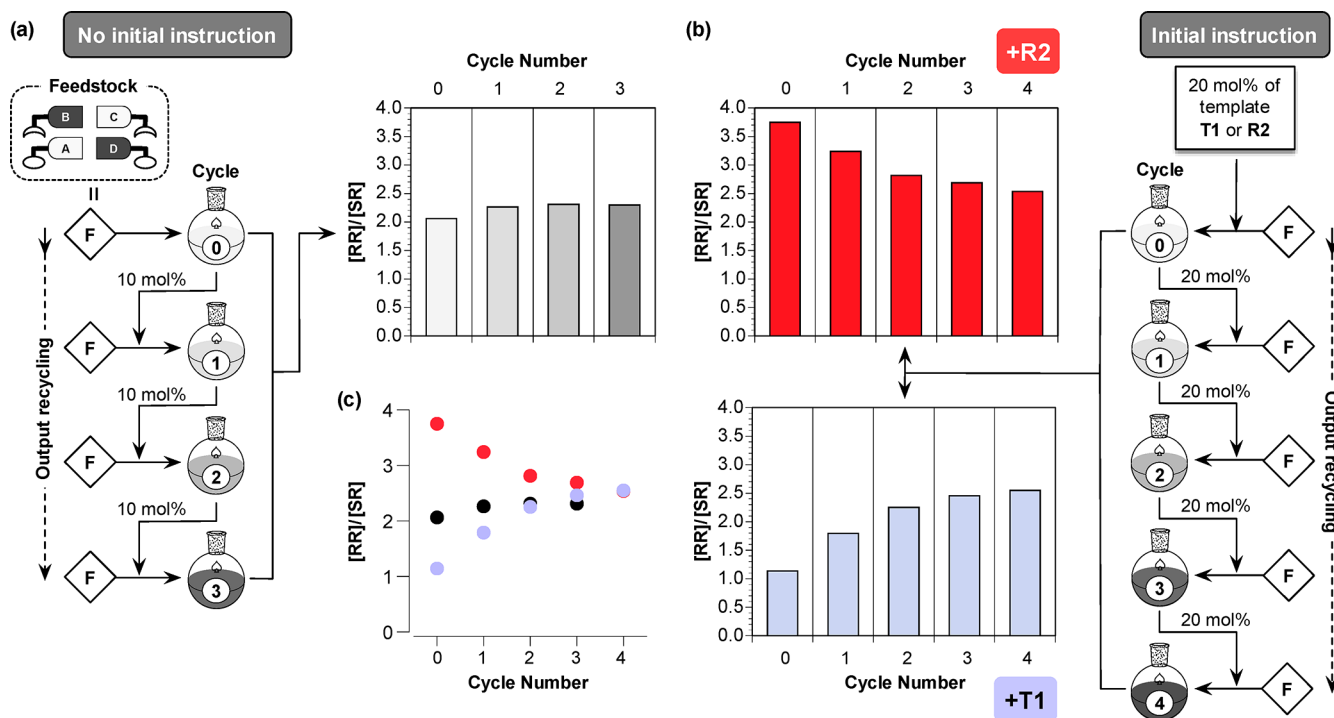


**Figure 3.** A set of serial transfer experiments demonstrates replicator persistence within the multicyclic network. The outcome of a reaction between reagents A to D ( $[A] = [B] = [C] = [D] = 10$  mM in  $CDCl_3$  at 283 K, monitored by 470 MHz  $^{19}F\{^1H\}$  NMR spectroscopy) can be used as the instructional input for a subsequent reaction. (a) In the absence of an initial instruction, the ratio  $[RR]/[SR]$  ( $= ([R1] + [R2])/([T1] + [T2])$ ) increases slightly across four cycles from 2.06 to 2.30 when 10 mol % of the output of one cycle is used as the instruction for the subsequent cycle. (b) The network can be biased toward either R1 and R2 or T1 and T2 by the addition of an instructional template to the initial reaction mixture (in this case, using either T1 or R2). However, the initial bias in the ratio  $[RR]/[SR]$  is eroded over the four subsequent cycles when 20 mol % of the output of one cycle is used as the instruction for the subsequent cycle. When the initial bias is provided by R2 (red bars),  $[RR]/[SR] = 3.75$  after cycle 0 and 2.54 after cycle 4. When the initial bias is provided by T1 (blue bars),  $[RR]/[SR] = 1.14$  after cycle 0 and 2.55 after cycle 4. (c) The data from the serial transfer experiments demonstrate that the ratio  $[RR]/[SR]$  converges to a single value irrespective of the starting input condition.

To this end, 10 mol % of the output from cycle 0 was added to a fresh solution of reagents A to D in  $CDCl_3$  such that  $[A] = [B] = [C] = [D] = 10$  mM. Once again, the formation of replicators T1, T2, R1, and R2 was monitored by 470 MHz  $^{19}F\{^1H\}$  NMR spectroscopy. This process was repeated a further two times. The results of these experiments (Figure 3a) reveal that, while the bias of the network toward reciprocal replicators does increase from cycle 0 (2.06:1) to cycle 3 (2.30:1), the largest change occurs between cycle 0 and cycle 1 (2.26:1). This observation indicates that the relative sizes of the four replicator populations are persistent under these conditions.

In order to probe the stability of the network toward larger perturbations, we next looked at the outcome of the recycling experiments where an instructional template was added in cycle 0 to generate an initial bias in the replicator populations. In this context, we performed two series of experiments (Figure 3b) whose basic setup was identical to that described previously. In the first series, a solution of reagents A to D in  $CDCl_3$  was prepared ( $[A] = [B] = [C] = [D] = 10$  mM, Figure 3b), and reciprocal replicator R2 was added as an instructional template at a concentration of 2 mM at  $t = 0$ . The addition of this template simulates a large perturbation in the replicator population from an exogenous source. The formation of the minimal replicators, T1 and T2, and the reciprocal replicators, R1 and R2, was assayed by 470 MHz  $^{19}F\{^1H\}$  NMR spectroscopy after complete consumption of starting materials.

After this time, the ratio of reciprocal replicators to self-replicators ( $[RR]/[SR]$ ) in this sample (Figure 3b, top, cycle 0) was significantly higher, at 3.75:1, than in the experiment (Figure 3a) where no instructional template had been added. However, as the output of one cycle was used as the instruction for the subsequent cycle, this bias was eroded rapidly and, after cycle 4, has settled at 2.54:1, a ratio close to the steady state reached in the case of experiments (Figure 3a) that were uninstructed initially.

When this process was repeated with self-replicator T1 as the initial instruction, the pattern of results was similar. A solution of reagents A to D in  $CDCl_3$  was prepared ( $[A] = [B] = [C] = [D] = 10$  mM, Figure 3b), and self-replicator T1 was added as an instructional template at a concentration of 2 mM at  $t = 0$ . The final ratio of reciprocal replicators to self-replicators ( $[RR]/[SR]$ ) in this sample (Figure 3b, bottom, cycle 0) was significantly lower, at 1.14:1, than that in the experiment (Figure 3a) where no instructional template had been added. Once again, as the output of one cycle was used as the instruction for the subsequent cycle, after cycle 4, the ratio settled at 2.55:1, a value close to the steady state reached in both the case of the recycling experiment (Figure 3a) that was uninstructed initially and that where R2 was used as the initial instruction.

These results are striking and demonstrate that this network of replicators possesses a natural, steady state composition (derived from the network connectivity) and that the network is resistant to changes away from this composition, at least

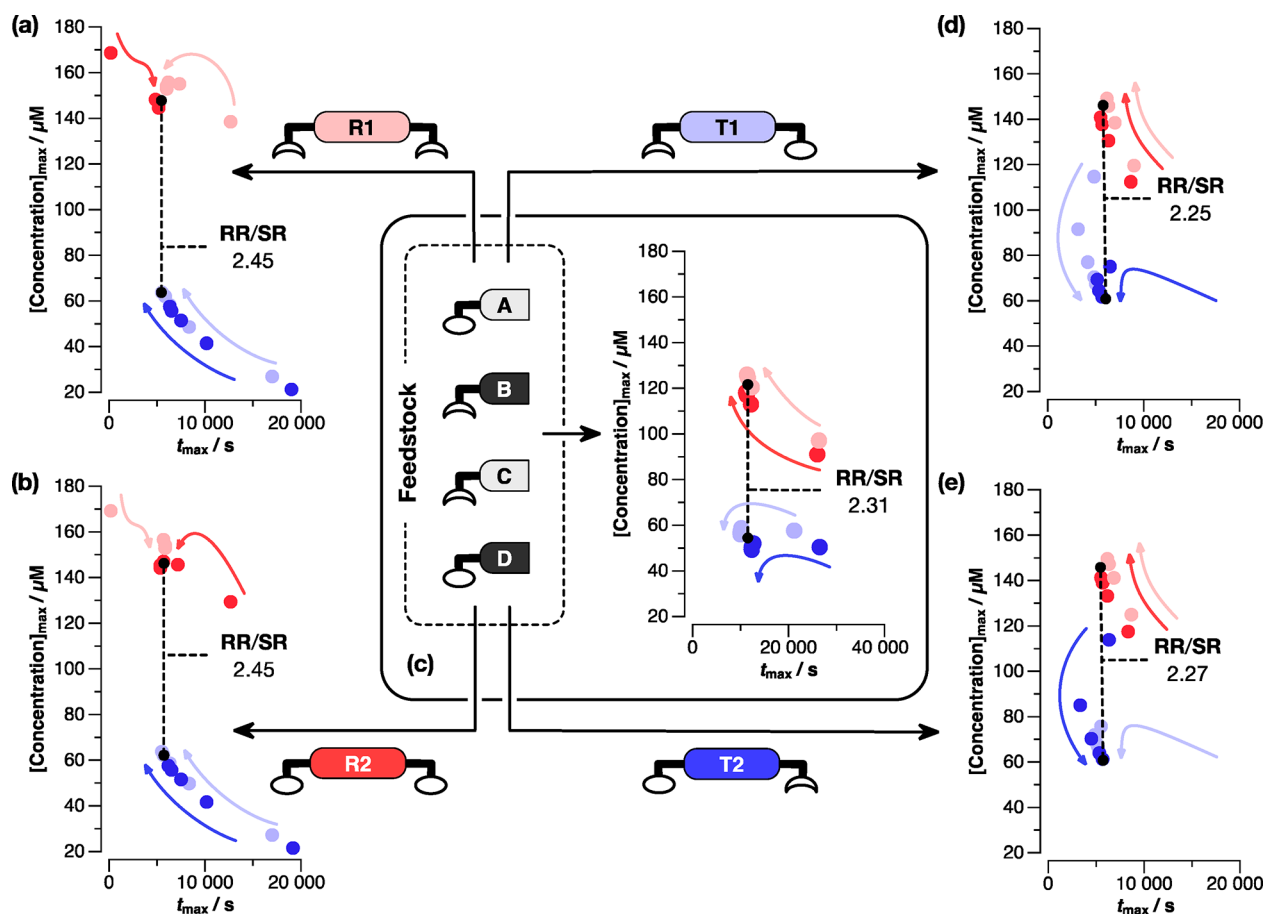


**Figure 4.** Data from the serial transfer experiments shown in Figure 3 can be reproduced using an appropriate kinetic model (Figure S8, Script S3). This kinetic model can be used to extract the behavior of the critical catalytically active ternary complexes,  $[A \cdot D \cdot R1]$ ,  $[B \cdot C \cdot R2]$ ,  $[A \cdot B \cdot T1]$ ,  $[C \cdot D \cdot T2]$ , as a function of both cycle number and time. The maximum concentrations of these catalytically active ternary complexes ( $[Concentration]_{\max}$ ) and the times at which these maxima are reached ( $t_{\max}$ ) converge as the cycle number increases when the multicyclic network is (a and b) instructed with reciprocal replicators, (c) uninstructed, and (d and e) instructed with self-replicators. The colored arrows indicate the paths described by the changes in these parameters for each ternary complex with increasing cycle number. As the system approaches convergence (black points), the composition of the material used as input for the next cycle becomes close to invariant. As a result,  $RR/SR = ([A \cdot D \cdot R1] + [B \cdot C \cdot R2]) / ([A \cdot B \cdot T1] + [C \cdot D \cdot T2])$  tends to a limiting condition and, therefore, the product distribution in subsequent cycles converges on a single  $[RR]/[SR]$  slowly.

within the confines of a well-stirred batch reactor where there is no continuous<sup>19</sup> inflow or outflow of material. In order to understand the origin of persistence of this network fingerprint, we employed a series of kinetic simulations using a mass action model (Script S3) based on solving ordinary differential equations (for full details, see Supporting Information, Section S1.2.4) that was capable of reproducing (Figure S8) the trends in the ratio of reciprocal to self-replicators observed in the recycling experiments that we carried out experimentally. The results of these simulations showed that the relative concentrations of the four catalytically active ternary complexes, namely,  $[A \cdot D \cdot R1]$ ,  $[B \cdot C \cdot R2]$ ,  $[A \cdot B \cdot T1]$ ,  $[C \cdot D \cdot T2]$  (Figure 1a), and how these concentrations vary with time, play a critical role in determining the output composition of the network.

Accordingly, we extracted from the simulation data for each cycle the maximum concentration of each ternary complex ( $[Concentration]_{\max}$ ) and the time point in each experiment at which this concentration maximum is achieved for each of the replicating templates ( $t_{\max}$ ). When the network is instructed initially with a reciprocal template (either R1 or R2), the locations of these maxima for the ternary complexes converge

rapidly (Figures 4a and b) toward two points in this concentration–time parameter space—one point for the reciprocal replicators and one point for the self-replicators—as the cycle number increases from 0 to 4. For example, in the data for the simulation where R1 is the instructing template (Figure 4a, top left), the concentration maxima for  $[A \cdot B \cdot T1]$  and  $[C \cdot D \cdot T2]$  are around 25  $\mu$ M and occur close to 20 000 s in cycle 0. As the cycle number increases (Figure 4a, blue-colored arrows), the maxima for T1 and T2 converge to a point around 60  $\mu$ M at 5500 s. Similarly, the maxima for R1 and R2 converge to a point around 150  $\mu$ M at 5500 s as the cycle number increases (Figure 4a, red-colored arrows). The ratio of these maxima for the ternary complexes ( $[A \cdot D \cdot R1] + [B \cdot C \cdot R2] / [A \cdot B \cdot T1] + [C \cdot D \cdot T2] = 2.45$ ) mirrors that of the final concentrations of the four replicators ( $([R1] + [R2]) / ([T1] + [T2])$ ) closely and is essentially invariant after four cycles. Similar convergence is also evident where the network is uninstructed (Figure 4c) or instructed initially with a self-replicating template (either T1 or T2, Figure 4d and e).

Once again, the locations of the maxima for the relevant ternary complexes converge rapidly toward two points in the concentration–time parameter space as the cycle number

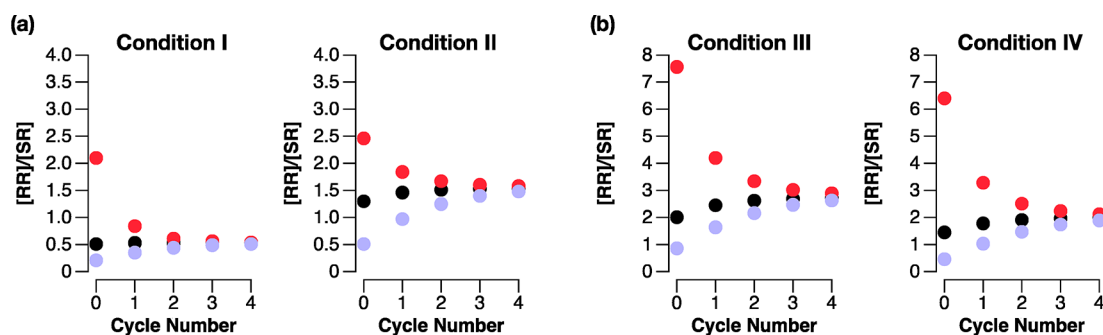


**Figure 5.** Simulated serial transfer experiments (see Script S3 for the original model) exploring how changes in (a) the initial concentrations of the starting materials A to D and (b) in the values of rate and duplex stability constants associated with the four template-directed pathways affect the network output. The  $[RR]/[SR]$  ( $[RR] = [R1] + [R2]$ ;  $[SR] = [T1] + [T2]$ ) ratio was simulated as a function of cycle number in the absence of template (black circles) or in the presence of preformed (2 mM) R2 (red circles) or T1 (blue circles) added at  $t = 0$  in cycle 0. The following parameters were changed in simulations I–IV relative to the original simulation (Figure S8): (a) condition I:  $[A] = 1$  mM; condition II:  $[A] = [B] = 5$  mM; (b) condition III:  $k_{\text{cat}}[C \cdot D \cdot T2] = 1.98 \times 10^{-3} \text{ s}^{-1}$ ,  $k_{\text{cat}}[B \cdot C \cdot R2] = 2.8 \times 10^{-3} \text{ s}^{-1}$ ; condition IV:  $[T1 \cdot T1] K_a^{\text{Duplex}} = 0.2 \times 10^6 \text{ M}^{-1}$ ,  $[T2 \cdot T2] K_a^{\text{Duplex}} = 20 \times 10^6 \text{ M}^{-1}$ ,  $[R1 \cdot R2] K_a^{\text{Duplex}} = 0.4 \times 10^6 \text{ M}^{-1}$ .

increases from 0 to 4 and the ratios of the maximum concentrations of ternary complexes mirrors closely the ratio of the final concentrations of the four replicators. After four cycles, the ratios are essentially invariant. These results indicate that the catalytic encoding present within this network—its connectivity defined by the interrelationships between the constituent replicating templates—stabilizes the output of the network. The network is therefore capable of recovering from significant perturbation to its composition, thereby preserving the innate composition of this system. The simulations shown in Figure 4 relate to starting conditions in which the concentrations of the starting materials are all equal (10 mM). In order to demonstrate that the persistence observed is a result of the network connectivity as opposed to the specific kinetic and thermodynamic properties of the replicators used, we performed two additional sets of simulations (for full details, see Supporting Information, Section S1.2.4).

In the first set of simulations, we explored<sup>20</sup> how variations in the concentrations of starting materials A to D affected the network output. In condition I (Figure 5a), the concentration of building block A is reduced to 1 mM, while the starting concentrations of B to D remain at 10 mM. Despite this drastic change, the network exhibits a trend in persistence that is qualitatively similar to that observed for the network when the starting condition is  $[A]$  to  $[D] = 10$  mM. This pattern is repeated (condition II, Figure 5a) when the concentrations of building blocks A and B are both reduced to 5 mM.

In the second set of simulations, we explored<sup>20</sup> the effect of changes in values of rate and duplex association constants associated with the four template-instructed pathways leading to R1, R2, T1, and T2. In condition III (Figure 5b), the efficiencies of the catalytic ternary complexes  $[C \cdot D \cdot T2]$  and  $[B \cdot C \cdot R2]$  are increased by a factor of 2. In condition IV (Figure 5b), the stabilities of the product duplexes are changed dramatically, by up to 20×. In both cases, the network exhibits trends in persistence that are qualitatively similar to those observed for the network when the original starting conditions are employed (Figure 3).

Taken together, the results of these simulations suggest strongly that the persistence observed experimentally is a direct result of the network connectivity as opposed to the specific kinetic and thermodynamic properties of the replicators used and the starting conditions employed.

## CONCLUSIONS

Replicator networks that embed replication processes provide experimental platforms for understanding the appearance on the early Earth of primitive “metabolic” pools capable of processing reagent pools in predefined and sustainable ways. Therefore, the establishment and maintenance of networks of replicators possessing connectivities that render them instructable by suitable template inputs can serve as models for these types of processes. In this work, we have created a replicator network whose behavior can be directed specifically by the introduction of instructional templates. Despite the fact that this network responds in predictable ways to instructions provided by these replicating templates, the results presented here show that there are compositional boundaries beyond which the network cannot be pushed by addition of a specific instruction provided by a replicating template. Within the environment of a well-stirred batch reactor, it is the connections between the compounds that make up the network—in terms of both their noncovalent interactions and their auto- and crosscatalytic properties—that encode resistance to changes in the composition of the network. As a consequence, this pool of replicators maintains a level of compositional stability and diversity, which can only be broken by placing the network in an environment where multiple steady states are possible.

## ASSOCIATED CONTENT

### Supporting Information

The Supporting Information is available free of charge on the ACS Publications website at DOI: 10.1021/jacs.9b06697.

Details of sample preparation, NMR analyses, kinetic simulations, and scripts (PDF)

## AUTHOR INFORMATION

### Corresponding Author

\*E-mail: d.philp@st-andrews.ac.uk.

### ORCID

Douglas Philp: 0000-0002-9198-4302

### Present Address

<sup>†</sup>(T.K. and D.P.) Department of Chemistry, Northwestern University, 2145 Sheridan Road, Evanston, Illinois 60208-3113, United States.



## Notes

The authors declare no competing financial interest. The research data supporting this publication can be accessed at <https://doi.org/10.17630/01de2c09-14e0-4e59-8111-d53f3e18c531> [Reference 21].

## ■ ACKNOWLEDGMENTS

This work was supported by the Engineering and Physical Sciences Research Council through Award EP/E017851/1 and through a Postgraduate Studentship to T.K. (EP/K503162/1), and by the University of St Andrews.

## ■ REFERENCES

- (1) (a) Islam, S.; Powner, M. Prebiotic systems chemistry: complexity overcoming clutter. *Chem.* **2017**, *2*, 470–501. (b) Peretó, J. Out of fuzzy chemistry: from prebiotic chemistry to metabolic networks. *Chem. Soc. Rev.* **2012**, *41*, 5394–5403. (c) Shapiro, R. Small molecule interactions were central to the origin of life. *Q. Rev. Biol.* **2006**, *81*, 105–126.
- (2) (a) Ritson, D. J.; Battilocchio, C.; Ley, S. V.; Sutherland, J. Mimicking the surface and prebiotic chemistry of early Earth using flow chemistry. *Nat. Commun.* **2018**, *9*, 1921. (b) Sutherland, J. D. The origin of life—out of the blue. *Angew. Chem., Int. Ed.* **2016**, *55*, 104–121. (c) Mann, S. The origins of life: old problems, new chemistries. *Angew. Chem., Int. Ed.* **2013**, *52*, 155–162. (d) Rauchfuss, H. In *Chemical Evolution and the Origin of Life*; Mitchell, T. N., Ed.; Springer: Berlin, 2008. (e) Luisi, P. L. *The Emergence of Life*; Cambridge University Press, 2006.
- (3) (a) Duim, H.; Otto, S. Towards open-ended evolution in self-replicating molecular systems. *Beilstein J. Org. Chem.* **2017**, *13*, 1189–1203. (b) Ashkenasy, G.; Hermans, T. M.; Otto, S.; Taylor, A. F. Systems chemistry. *Chem. Soc. Rev.* **2017**, *46*, 2543–2554. (c) Miljanić, O. S. Small-molecule systems chemistry. *Chem.* **2017**, *2*, 502–524. (d) de la Escosura, A.; Briones, C.; Ruiz-Mirazo, K. The systems perspective at the crossroads between chemistry and biology. *J. Theor. Biol.* **2015**, *381*, 11–22. (e) Mattia, E.; Otto, S. Supramolecular systems chemistry. *Nat. Nanotechnol.* **2015**, *10*, 111–119. (f) Ruiz-Mirazo, K.; Briones, C.; de la Escosura, A. Prebiotic systems chemistry: new perspectives for the origins of life. *Chem. Rev.* **2014**, *114*, 285–366.
- (4) (a) Tirard, S. Origin of life and definition of life, from Buffon to Oparin. *Origins Life Evol. Biospheres* **2010**, *40*, 215–220. (b) Benner, S. A. Defining life. *Astrobiology* **2010**, *10*, 1021–1030. (c) Lazcano, A. What is life? *Chem. Biodiversity* **2008**, *5*, 1–15. (d) Cleland, C. E.; Chyba, C. F. Defining ‘life’. *Origins Life Evol. Biospheres* **2002**, *32*, 387–393. (e) Joyce, G. F. Foreword. In *Origins of Life: The Central Concepts*; Deamer, D. W.; Fleischaker, G., Eds.; Jones and Bartlett: Boston, 1994; pp xi–xii. (f) Schrödinger, E. *What Is Life?*; Cambridge University Press: Cambridge, 1944.
- (5) (a) Kosikova, T.; Philp, D. Exploring the emergence of complexity using synthetic replicators. *Chem. Soc. Rev.* **2017**, *46*, 7274–7305. (b) Bissette, A. J.; Fletcher, S. P. Mechanisms of autocatalysis. *Angew. Chem., Int. Ed.* **2013**, *52*, 12800–12826. (c) Philp, D.; Huck, J. *Supramolecular Chemistry: From Molecules to Nanomaterials*; John Wiley & Sons, Ltd.: New York, 2012; Vol. 4, pp 1415–1445. (d) Vidonne, A.; Philp, D. Making molecules make themselves—the chemistry of artificial replicators. *Eur. J. Org. Chem.* **2009**, *2009*, 593–610. (e) Dadon, Z.; Wagner, N.; Ashkenasy, G. The road to non-enzymatic molecular networks. *Angew. Chem., Int. Ed.* **2008**, *47*, 6128–6136. (f) Patzke, V.; von Kiedrowski, G. Self-replicating systems. *ARKIVOC* **2007**, *46*, 293–310. (g) Paul, N.; Joyce, G. F. Minimal self-replicating systems. *Curr. Opin. Chem. Biol.* **2004**, *8*, 634–639. (h) Von Kiedrowski, G. Minimal replicator theory I: parabolic versus exponential growth. *Bioorg. Chem. Front.* **1993**, *3*, 113–146.
- (6) (a) Robertson, C. C.; Kosikova, T.; Philp, D. An environmentally responsive reciprocal replicating network. *J. Am. Chem. Soc.* **2018**, *140*, 6832–6841. (b) Sadownik, J. W.; Kosikova, T.; Philp, D. Generating system-level responses from a network of simple synthetic replicators. *J. Am. Chem. Soc.* **2017**, *139*, 17565–17573. (c) Kosikova, T.; Philp, D. A critical cross-catalytic relationship determines the outcome of competition in a replicator network. *J. Am. Chem. Soc.* **2017**, *139*, 12579–12590. (d) Bottero, I.; Huck, J.; Kosikova, T.; Philp, D. A synthetic replicator drives a propagating reaction–diffusion front. *J. Am. Chem. Soc.* **2016**, *138*, 6723–6726. (e) Kosikova, T.; Hassan, N. I.; Cordes, D. B.; Slawin, A. M. Z.; Philp, D. Orthogonal recognition processes drive the assembly and replication of a [2]rotaxane. *J. Am. Chem. Soc.* **2015**, *137*, 16074–16083. (f) Kassianidis, E.; Philp, D. Design and implementation of a highly selective minimal self-replicating system. *Angew. Chem., Int. Ed.* **2006**, *45*, 6344–6348.
- (7) For examples of synthetic replicating systems based on oligonucleotides, see: (a) Plöger, T. A.; von Kiedrowski, G. A self-replicating peptide nucleic acid. *Org. Biomol. Chem.* **2014**, *12*, 6908–6914. (b) Lincoln, T. A.; Joyce, G. F. Self-sustained replication of an RNA enzyme. *Science* **2009**, *323*, 1229–1232. (c) Paul, N.; Joyce, G. F. A self-replicating ligase ribozyme. *Proc. Natl. Acad. Sci. U. S. A.* **2002**, *99*, 12733–12740. (d) von Kiedrowski, G.; Wlotzka, B.; Helbing, J.; Matzen, M.; Jordan, S. Parabolic growth of a self-replicating hexadeoxynucleotide bearing a 3′-5′-phosphoramidate linkage. *Angew. Chem., Int. Ed. Engl.* **1991**, *30*, 423–426. (e) von Kiedrowski, G. A self-replicating hexadeoxynucleotide. *Angew. Chem., Int. Ed. Engl.* **1986**, *25*, 932–935.
- (8) For examples of synthetic replicating systems based on peptides, see: (a) Altay, M.; Altay, Y.; Otto, S. Parasitic behavior of self-replicating molecules. *Angew. Chem., Int. Ed.* **2018**, *139*, 10564–10568. (b) Sadownik, J. W.; Mattia, E.; Nowak, P.; Otto, S. Diversification of self-replicating molecules. *Nat. Chem.* **2016**, *8*, 264–269. (c) Colomb-Delsuc, M.; Mattia, E.; Sadownik, J. W.; Otto, S. Exponential self-replication enabled through a fibre elongation/breakage mechanism. *Nat. Commun.* **2015**, *6*, 7427. (d) Dadon, Z.; Wagner, N.; Alasibi, S.; Samiappan, M.; Mukherjee, R.; Ashkenasy, G. Competition and cooperation in dynamic replication networks. *Chem. - Eur. J.* **2015**, *21*, 648–654. (e) Samiappan, M.; Dadon, Z.; Ashkenasy, G. Replication NAND gate with light as input and output. *Chem. Commun.* **2011**, *47*, 710–712. (f) Carnall, J. M. A.; Waudby, C. A.; Belenguer, A. M.; Stuart, M. C. A.; Peyralans, J. J. -P.; Otto, S. Mechanosensitive self-replication driven by self-organization. *Science* **2010**, *327*, 1502–1506. (g) Issac, R.; Chmielewski, J. Approaching exponential growth with a self-replicating peptide. *J. Am. Chem. Soc.* **2002**, *124*, 6808–6809. (h) Saghatelian, A.; Yokobayashi, Y.; Soltani, K.; Ghadiri, M. R. A chiroselective peptide replicator. *Nature* **2001**, *409*, 797–801. (i) Lee, D. H.; Granja, J. R.; Martinez, J. A.; Severin, K.; Ghadiri, M. R. A self-replicating peptide. *Nature* **1996**, *382*, 525–528.
- (9) For examples of synthetic replicating systems based on small organic molecules, see: (a) Morrow, S. M.; Colomer, I.; Fletcher, S. P. A chemically fueled self-replicator. *Nat. Commun.* **2019**, *10*, 1011. (b) Colomer, I.; Morrow, S. M.; Fletcher, S. P. A transient self-assembling self-replicator. *Nat. Commun.* **2018**, *9*, 2239. (c) Taylor, J. W.; Eghtesadi, S. A.; Points, L. J.; Cronin, L. Autonomous model protocell division driven by molecular replication. *Nat. Commun.* **2017**, *8*, 237. (d) Kindermann, M.; Stahl, I.; Reimold, M.; Pankau, W. M.; von Kiedrowski, G. Systems chemistry: kinetic and computational analysis of a nearly exponential organic replicator. *Angew. Chem., Int. Ed.* **2005**, *44*, 6750–6755. (e) Wang, B.; Sutherland, I. O. Self-replication in a Diels–Alder reaction. *Chem. Commun.* **1997**, 1495–1496. (f) Rotello, V.; Hong, J.-I.; Rebek, J., Jr. Sigmoidal growth in a self-replicating system. *J. Am. Chem. Soc.* **1991**, *113*, 9422–9423.
- (10) Sadownik, J. W.; Philp, D. A simple synthetic replicator amplifies itself from a dynamic reagent pool. *Angew. Chem., Int. Ed.* **2008**, *47*, 9965–9970.
- (11) (a) Helwig, B.; van Sluijs, B.; Pogodaev, A. A.; Postma, S. G. J.; Huck, W. T. S. Bottom-up construction of an adaptive enzymatic reaction-network. *Angew. Chem., Int. Ed.* **2018**, *57*, 14065–14069. (b) Ashkenasy, G.; Dadon, Z.; Alesebi, S.; Wagner, N.; Ashkenasy, N.



Building logic into peptide networks: bottom-up and top-down. *Isr. J. Chem.* **2011**, *51*, 106–117.

(12) Postma, S. G. J.; te Brinke, D.; Vialshin, I. N.; Wong, A. S. Y.; Huck, W. T. S. A trypsin-based bistable switch. *Tetrahedron* **2017**, *73*, 4896–4900.

(13) (a) Cafferty, B. J.; Wong, A. S. Y.; Semenov, S. N.; Belding, L.; Gmur, S.; Huck, W. T. S.; Whitesides, G. M. Robustness, entrainment, and hybridization in dissipative molecular networks, and the origin of life. *J. Am. Chem. Soc.* **2019**, *141*, 8289–8295. (b) Pogodaev, A. A.; Wong, A. S. Y.; Huck, W. T. S. Photochemical control over oscillations in chemical reaction networks. *J. Am. Chem. Soc.* **2017**, *139*, 15296–15299. (c) Semenov, S. N.; Kraft, L. J.; Ainla, A.; Zhao, M.; Baghbanzadeh, M.; Campbell, V. E.; Kang, K.; Fox, J. M.; Whitesides, G. M. Autocatalytic, bistable, oscillatory networks of biologically relevant organic reactions. *Nature* **2016**, *537*, 656–660. (d) Wagner, N.; Alasibi, S.; Peacock-Lopez, E.; Ashkenasy, G. Coupled oscillations and circadian rhythms in molecular replication networks. *J. Phys. Chem. Lett.* **2015**, *6*, 60–65. (e) Fuji, T.; Rondelez, Y. Predator–prey molecular ecosystems. *ACS Nano* **2013**, *7*, 27–34. (f) Montagne, K.; Plasson, R.; Sakai, Y.; Fujii, T.; Rondelez, Y. Programming an *in vitro* DNA oscillator using a molecular networking strategy. *Mol. Syst. Biol.* **2011**, *7*, 466.

(14) (a) Skorb, E. V.; Semenov, S. N. Mathematical analysis of a prototypical autocatalytic reaction network. *Life* **2019**, *9*, 42. (b) Hordijk, W.; Steel, M.; Dittrich, P. Autocatalytic sets and chemical organizations: modelling self-sustaining reaction networks at the origin of life. *New J. Phys.* **2018**, *20*, 01501. (c) Yeates, J. A. M.; Hilbe, C.; Zwick, M.; Nowak, M. A.; Lehman, N. Dynamics of prebiotic RNA reproduction illuminated by chemical game theory. *Proc. Natl. Acad. Sci. U. S. A.* **2016**, *113*, 5030–5035. (d) Vasas, V.; Szathmáry, S. M. Lack of evolvability in self-sustaining autocatalytic networks *constraints* metabolism-first scenarios for the origin of life. *Proc. Natl. Acad. Sci. U. S. A.* **2010**, *107*, 1470–1475. (e) Hordijk, W.; Hein, J.; Steel, M. Autocatalytic sets and the origin of life. *Entropy* **2010**, *12*, 1733–1742.

(15) (a) Kassianidis, E.; Pearson, R. J.; Wood, E. A.; Philp, D. Designing instructable networks using synthetic replicators. *Faraday Discuss.* **2010**, *145*, 235–254. (b) Kassianidis, E.; Philp, D. Reciprocal template effects in a simple synthetic system. *Chem. Commun.* **2006**, 4072–4074.

(16) The adjective “system-level”, when used in conjunction with nouns such as “behavior”, “effect”, or “properties”, is used to represent effects that arise as a result of the presence of interactions and reactions within the system under study. These indirect connections between members in a network result in the observation of effects that are not expressed in the absence of these catalytic and interactional inter-relationships.

(17) Becker, S.; Schneider, C.; Okamura, H.; Crisp, A.; Amato, T.; Dejme, M.; Carell, T. Wet–dry cycles enable the parallel origin of canonical and non-canonical nucleosides by continuous synthesis. *Nat. Commun.* **2018**, *9*, 163.

(18) (a) Hordijk, W.; Vaidya, N.; Lehman, N. Serial transfer can aid the evolution of autocatalytic sets. *J. Syst. Chem.* **2014**, *5*, 4. (b) Joyce, G. F. Evolution in an RNA world. *Cold Spring Harbor Symp. Quant. Biol.* **2009**, *74*, 17–23.

(19) Wagner, N.; Hochberg, D.; Peacock-Lopez, E.; Maity, I.; Ashkenasy, G. Open prebiotic environments drive emergent phenomena and complex behaviour. *Life* **2019**, *9*, 45.

(20) For detailed descriptions of the additional simulations exploring how changes in the initial concentrations of the starting materials A to D and in the values of rate and duplex association constants associated with the four template-directed pathways affect the network output, see Figure S9, Figure S10, and Table S1.

(21) Huck, J.; Kosikova, T.; Philp, D. Compositional persistence in a multicyclic network of synthetic replicators (dataset). *Dataset. University of St. Andrews Research Portal*, 2019 DOI: [10.17630/01de2c09-14e0-4e59-8111-d53f3e18c531](https://doi.org/10.17630/01de2c09-14e0-4e59-8111-d53f3e18c531).